High-Resolution Spectroscopic Studies of C_{60} and $C_6H_7^+$: Molecules of Fundamental Spectroscopic and Astrochemical Importance

Brian E. Brumfield
Preliminary Examination
November 15, 2007
2:00 PM CLSL 133A

I. Current Experimental Work Overview

I am currently involved in an experiment to acquire a cold rotationally resolved gas phase spectrum of buckminsterfullerene (C_{60}) in the mid-IR. This is an interesting project from a fundamental spectroscopic point of view because it will represent the heaviest and most symmetric molecule ever studied in the gas phase. As a consequence of its high symmetry, and composition of 60 ^{12}C bosons, there will be missing rotational levels which will in turn yield missing transitions in the vibrational band.[1,2]

A high-resolution gas phase spectrum is also interesting from an astrochemical /astrophysical perspective. C_{60} was originally discovered in experiments seeking to understand long carbon chain chemistry in the interstellar medium (ISM) and circumstellar shells.[3] Since its initial discovery, indirect evidence has been found for the existence of C_{60} in space,[4,5] but direct evidence for C_{60} in the interstellar medium will require positive identification in a spectroscopic search, and a high resolution laboratory spectrum of C_{60} is essential for such a search.

We have not yet obtained a high resolution spectrum of C_{60}, but significant progress has been made in the experiment, allowing for the collection of high-resolution cavity ringdown (CRD) spectra. I have been responsible for learning how to scan the continuous wave Fabry-Perot quantum cascade laser (cw-FP-QCL) used in the experiment, and the assignment/analysis of the first high-resolution spectrum of the ν_8 band of methylene bromide (CH_2Br_2).

I. 1. Experimental Background

The general experimental layout is provided in Figure 1 (see attached figures at end of document). The primary goal of the sample preparation portion of the experiment is to generate cold gas phase molecules from a solid sample by using a high temperature oven coupled to a supersonic pinhole expansion. The high temperature oven can attain temperatures >600ºC for several hours, and this makes it possible to generate a sufficient concentration of gas phase molecules from low vapor pressure solids such as C_{60}. The hot vapor from the sample is then

forced through a pinhole by a high pressure of inert carrier gas entering through the inlet gas line, generating a seeded supersonic expansion that provides rotational and vibrational cooling of the hot gas phase sample.[6,7]

The CRD collection scheme employed in this work was originally developed by Romanini et al.[8,9] and has been successfully implemented by other research groups.[10,11,12] In our experimental set-up, a cw-FP-QCL operating ~8.5 μm is passed through a set of collimation optics and then an acousto-optic modulator (AOM). The first order diffraction from the AOM passes through a pair of mode matching optics to effectively couple light into the TEM_{00} mode of the high finesse optical cavity formed by two highly reflective mirrors. A piezoelectric transducer (PZT) dithers the position of one of the cavity mirrors, effectively sweeping the cavity modes by at least one free spectral range (FSR). When a cavity mode is swept into resonance with the laser frequency, a sharp build-up of intracavity power occurs. Once the light intensity leaking out of the cavity measured by the detector reaches a threshold value, the driver to the AOM is turned off and light injection into the cavity is suppressed. The decay rate of light leaking out of the cavity is directly proportional to the absorption losses due to the medium in the cavity and the mirror losses. By measuring this decay rate it is possible to determine the absolute absorption coefficient for the cavity and medium at the specified laser frequency. Using this CRD collection scheme in the McCall laboratory it has been possible to achieve noise equivalent absorption (NEA) coefficients as small as $\sim 2 \times 10^{-9}$ cm^{-1}. After integrating a sufficient number of ringdown events, the laser frequency is then stepped. During the process of acquiring CRD spectra a portion of the QCL output is split off to a reference path through an absorption cell filled with N_2O to provide absolute frequency calibration.

A critical part of the cw-CRDS spectrometer is the cw-FP-QCL. QCLs are composed of repeated quantum well structures designed by periodic layering of doped semiconductor materials.[13] When a current is applied to the device electrons are injected into the multi-

quantum well (MQW) structure. The electrons may then relax through each successive period with the potential of emitting a photon by either spontaneous or stimulated emission. By controlling the thickness and composition of the semiconductor layering it has been possible to produce QCLs lasing anywhere from 3 to 24 μm, with cw laser power output power as high as tens of milliwatts.[14] When compared to the low power output (<1 mW), and limited availability of lead salt diode lasers >5 μm, the QCL is a superior choice for our experiment. However, the device is still in the process of being commercialized, and has only been implemented in two experimental cw-CRD spectrometers.[10,11]

The cw-FP-QCL employed in our spectrometer is housed in a liquid nitrogen cooled cryostat. This is necessary to disperse the roughly 10 Watts of heat generated by the laser during cw operation. The internal mounting of the laser inside the cryostat had to be radically altered to afford mechanical stability of the laser while maintaining an adequate thermal connection. These goals were achieved by connecting the laser submount to the outside of the cryostat and using folded sheets of copper ribbon to maintain a thermal connection to the cryostat cold head. Frequency tuning of the laser is accomplished by manipulating the temperature and current sourced to the device. During scanning, a temperature controller is used to maintain the device at a stable temperature. A power supply is then used to alter the current in a controlled step-wise fashion during CRD acquisition. In this fashion, it is possible to achieve 1-2 cm^{-1} mode-hop free coverage at a single temperature.

I. 2. Methylene Bromide Analysis

In order for the C_{60} experiment to be successful, we need to generate a sample with a low rotational and vibrational temperature. To carry out a test of the effectiveness of the supersonic free jet expansion, methylene bromide (CH_2Br_2) was chosen as a test molecule because it has a vibrational band (ν_8) that falls within the frequency coverage of the cw-FP-QCL. Unfortunately, the only spectra of the band in the literature have been taken at low resolution and show only the

band contours of the P, Q, and R branches.[15,16] In order to interpret how effective the pinhole source is at cooling molecules seeded in the expansion, the high resolution spectra of the ν_8 band must be assigned. Correct assignment will then yield the molecular constants necessary to generate simulated spectra at a variety of temperatures.

The task of accurately assigning the ν_8 band is complicated by the 1:1 isotopic ratio of ^{79}Br to ^{81}Br, which leads to a 1:2:1 ratio of the $CH_2{}^{79}Br_2$, $CH_2{}^{79}Br^{81}Br$, and $CH_2{}^{81}Br_2$ isotopomers. The experimental spectrum is therefore comprised of the spectra of three molecules with slightly different rotational constants, vibrational band centers, and intensity alternation due to differences in point group symmetry.

The top trace in Figure 2 represents a portion of the spectrum that has been acquired from 1196.35 to 1197.00 cm^{-1}. The laser was stepped in ~54 MHz increments during the acquisition of this scan, and frequency calibration was carried out using five N_2O reference lines.

I carried out the process of assigning all three bands of the methylene bromide isotopomers using a spectral fitting program called Pgopher.[17] It was possible to fix the ground state rotational constants to their available literature values obtained through microwave work.[18,19] The next step was an iterative process of assignment starting with the Q-branch subbands and low J P-branch subbands belonging to the $CH_2{}^{79}Br^{81}Br$ isotopomer. In the end I was able to make tentative assignments for 42 $CH_2{}^{79}Br^{81}Br$ transitions, 33 $CH_2{}^{81}Br_2$ transitions, and 17 $CH_2{}^{79}Br_2$ transitions. The linear least squares fit for all three sets fell around ~27 MHz; half of the ~ 54 MHz frequency step size. The upper state distortion constants were ill defined because of inadequate experimental resolution and mode-hop free spectral coverage, but it was possible to obtain definite values for the upper state rotational constants in the fit. The lower inverted trace in Figure 2 represents a composite simulation that I generated for all three isotopomers at 20K using parameters determined from the tentatively assigned set of transitions.

II. Future Experimental Work Overview

In my future work, I will focus on the acquisition and analysis of mid-IR high resolution spectra of a vibrational band of protonated benzene, also known as the benzenium ion ($C_6H_7^+$). The benzenium ion represents the prototypical arenium ion intermediate in electrophilic aromatic substitution (EAS) reactions.[20] Being a key reaction intermediate, there is an intense interest in the structure and intramolecular dynamics of this molecular ion, as is evident from the variety of applied experimental techniques and computational studies that have been carried out: NMR work in cold superacid media[21,22], infrared photodissociation spectroscopy[23,24,25], radiolytic methods[26], mass spectroscopy[27,28], and theoretical computational work.[29,30] These studies have established the equilibrium structure for the molecular ion, and have explored the energy barrier for the intramolecular phenomenon of proton "ring-walk." The "ring-walk" mechanism occurs because the energy barrier to proton migration is sufficiently low that the proton can easily tunnel through the barrier. This tunneling will manifest itself as distinct spectroscopic splittings under high-resolution gas phase studies of the rovibrational bands of the ion. A detailed analysis of the rich tunneling splitting in the spectrum will allow accurate determination of the ring-walk barrier, and will pave the way for future studies probing mono-substituted benzenium ions to study the influence of ortho/para and meta directors on the tunneling barriers.

The benzenium ion is of astrochemical interest as an intermediate in proposed synthetic paths for benzene in dense interstellar clouds and proto-planetary nebula (PPN).[31,32] Benzene in the interstellar and circumstellar medium is a likely building block for polycyclic aromatic hydrocarbons (PAHs), which are implicated carriers of the diffuse interstellar bands (DIBs) and the unidentified infrared bands (UIBs). A positive detection of benzene has already been established in the PPN CRL 618,[33] bolstering the case for formation of complex PAHs in PPN. A combination differences analysis of the high-resolution rovibrational spectra can provide knowledge of the ground state energy level structure, and enable a radio astronomical search.

High resolution rovibrational spectra of the benzenium ion will be made possible with the sensitive cooled resolved ion beam spectroscopy (SCRIBES) instrument currently under development in the McCall lab. The SCRIBES instrument will combine the sub-Doppler line narrowing phenomenon of acceleration cooling in fast ion beams with cw-CRDS.

II. 1. Experimental: The SCRIBES Instrument

High-resolution direct absorption laser spectroscopy of molecular ions in plasmas is fraught with significant difficulties: spectral complexity due to high T_{rot} and T_{vib} in the discharge plasma, broad linewidths due Doppler broadening at high T_{trans}, and weak molecular ion absorptions compared to stronger absorption signals from neutrals due to their abundance in the plasma. Pulling the relatively weaker molecular ion absorption signals out of a strong neutral "background" was resolved in the early 1980's with the development of the velocity modulation technique.[34] In this technique the polarity of the discharge generating the plasma is rapidly flipped (~kHz) causing the molecular ion absorption features to blue and red Doppler shift at the discharge polarity inversion frequency. A lock-in amplifier can then be used to extract the signal of spectral features that are modulated at the polarity inversion discharge frequency.

Velocity modulation does not resolve the linewidth or spectral complexity issues of carrying out direct absorption spectroscopy in hot discharge plasmas. In the late 1980's and early 1990's, the direct laser absorption spectroscopy in fast ion beams (DLASFIB) method was developed in the Saykally group at Berkeley in an attempt to surmount these issues.[35,36,37] The DLASFIB instrument was able to combat broad linewidths by utilizing the acceleration cooling effect in fast ion beams probed along the parallel direction. Briefly, acceleration cooling is a velocity "bunching" phenomenon that occurs by generating molecular ions in a discharge source that is floated at a high positive (~kV) potential.[38,39] Ions are born in the discharge source with additional potential energy due to interaction with the float voltage field, and when exiting the source this potential energy is converted to kinetic energy. This addition of energy leads to a

reduction in the longitudinal velocity spread of the ions. Acceleration cooling can be used to achieve sub-Doppler linewidths of ~20 MHz. In addition to acceleration cooling, a mass spectrometer was present at the end of the ion beam system allowing mass identification of spectral carriers present in the ion beam. Despite these achievements the DLASFIB technique was abandoned due to difficulties implementing a supersonic expansion discharge source.

The SCRIBES instrument under development in the McCall lab represents a substantial improvement over the DLASFIB instrument by making use of a broadly tunable difference frequency generation laser system to carry out cw-CRDS in a fast ion beam. Figure 3 shows the fundamental layout of the SCRIBES instrument. The first chamber will house a floated cw supersonic expansion discharge source responsible for generating a fast cold molecular ion beam. In the source a discharge will be generated in a flowing benzene/H_2/rare gas mixture to create sufficient H_3^+ to protonate benzene. A skimmer positioned directly after the source will separate the source chamber from the chamber housing the ion optics and the first quadrupole. The source chamber will be pumped by a two stage roots blower backed with a rotary vane pump (~7500 cfm). This will facilitate the removal of the enormous amount of gas introduced by the cw source, and will maintain a low background pressure for the supersonic expansion.

After the ion beam passes through the skimmer, it is collimated by a pair of electrostatic lenses before entering the first quadrupole. The quadrupole will turn the ion beam by 90º into the drift region of the instrument while the remaining neutrals pass straight through. The acceleration cooling should provide sub-Doppler linewidths ~20 MHz, as attainable with the DLASFIB instrument. The ion beam in the drift region lies along the axis of a high finesse cavity and is overlapped with coupled light from a tunable mid-IR difference frequency generation (DFG) system. The DFG system is capable of frequency coverage from ~2000 cm^{-1} to 5000 cm^{-1}, and the light is generated by coupling the output from a fixed frequency cw Nd:YAG laser with a tunable cw Ti:Sapph laser into a periodically poled lithium niobate crystal

(PPLN). Because light in the cavity will propagate both parallel, and anti-parallel all transitions will be Doppler split into a doublet by their velocity in the drift region. This frequency separation will provide a measure of the mass of the spectral carrier.

The weak band strength of C-H stretching modes in the benzenium ion presents a challenge to the sensitivity of conventional cw-CRDS. To increase the sensitivity of the SCRIBES instrument, it will be necessary to implement high-repetition rate cw-CRDS. In high-repetition rate ringdown, the frequency of the laser is locked to the high-finesse cavity. By actively locking the laser to the cavity the dead-time experienced during the piezo sweep in a traditional cw-CRDS experiment is removed. The rate of ringdown occurrences is then controlled by rapidly switching on and off the AOM driver. Using this technique a CRD spectrometer with an acquisition rate of 10 kHz has been built, and a long-term minimum detectable absorption of 9.0×10^{-11} cm^{-1} $Hz^{-1/2}$ has been obtained.[40]

The second quadrupole will turn the ion beam into a time of flight mass spectrometer (TOF-MS). The TOF-MS will provide information about the mass of the spectral carriers in the beam, and can be compared with Doppler splittings in the ringdown spectra. The TOF-MS can also aid attempts to optimize flow mixture composition and source conditions to maximize production of a desired target molecular ion.

II. 2. Influence of Intramolecular Dynamics on Benzenium Ion Spectra

The benzenium ion represents a fluxional carbocation system where the occurrence of tunneling will manifest itself as distinct spectroscopic splittings when studied under high-resolution. The addition of a seventh hydrogen to the benzene ring leads to a C_{2v} equilibrium structure (1) shown in figure 4. A bridged intermediate of C_s symmetry (2) provides the path for the proton to be transferred from one carbon to another on the ring as illustrated by structure (3). The energy barrier for this process has been estimated to be 10±1 kcal/mol, and is low enough that rapid tunneling leads to a proton "ring-walk" motion.

Because of this fluxional behavior, there exist 2520 equivalent potential minima, and due to tunneling the energy levels for the rigid C_{2v} equilibrium structure are split. To gain a greater understanding of the problem, I propose the acquisition of high resolution spectra of the symmetric and asymmetric $-CH_2$ streches at 2807 and 2801 cm^{-1} respectively using the SCRIBES instrument.

I have carried out a group theory analysis of the benzenium ion to gain a greater insight into the degree of splitting of the ground rotational levels. This entailed generating the S_7^* character table using a freely available discrete algrebra computation package called GAP.[41] With the S_7^* character table it was possible to build a correlation table relating symmetry representations from the rigid benzenium ion structure to symmetry representations for the non-rigid benzenium ion structure.[42,43] Determination of the symmetry labels spanning the nuclear spin representation allowed for an analysis of the number of Pauli allowed states given the rotational level state symmetries, and this revealed that each asymmetric top rotational level is split into six levels.

Though group theory can give an absolute value for the number of splittings, it cannot provide an order of magnitude estimate for the splitting separation. To provide a gross estimate of the tunneling splittings I have used the tunneling rate equation for a symmetric double well potential, and varied the potential barrier from 11 kcal/mol to 5.5 kcal/mol. This analysis has revealed that tunneling in the ground state will lie within an order of magnitude between $1x10^{-5}$ cm^{-1} to $1x10^{-4}$ cm^{-1}, and that the frequency separation of the splittings will be largely dominated by the degree of tunneling in the excited vibrational state. Carrying out a similar analysis for the vibrational excited state is not as straightforward because neither the symmetric or asymmetric stretching mode couple directly into barrier crossing. Coriolis coupling could permit a fraction of the overall energy placed into the mode to be involved in the barrier crossing motion, and I

have chosen to treat this as a reduction in the barrier height for tunneling. A couple hundred wavenumber reduction in the barrier height yields splittings on the order of ~10 MHz.

Using the group theory analysis, and the double well tunneling frequency model, some general comments can be made about the possible appearance of a high resolution spectrum obtained using the SCRIBES instrument. Depending on how the effective potential barrier scales the resulting spectrum could be anywhere from that of a normal near oblate asymmetric to a spectrum with resolvable tunnel splitting separations that are larger than the linewidth for the transitions. Even if the frequency separation due to splitting is close to that of the linewidth for the transitions the peak shapes will still reflect the spin statistical weights for the split levels in the ground state. This will permit a lineshape analysis and the extraction of knowledge regarding the height of the effective potential barrier.

Conclusion

Overall, significant progress has been made in the last year in the C_{60} experiment. Currently I am working to achieve optical isolation of the QCL to decrease laser mode hops. Once optical isolation has been achieved it will then be possible to reliably scan over the region where the C_{60} vibrational band is located.

The benzenium ion project cannot currently be started until the SCRIBES instrument is built and characterized. Currently the source chamber, first quadrupole, and drift region are in place, and an uncooled cathode discharge source and the DFG system are operational. Once the initial characterization of the instrument is completed I intend to test the supersonic discharge source to gauge the beam current of $C_6H_7^+$ that I can generate.

The C_{60} and proposed $C_6H_7^+$ projects represent intriguing research problems that highlight the influence molecular symmetry has on the structure of a vibrational band. Both of these projects will also provide the necessary information to enable spectroscopic searches in space.

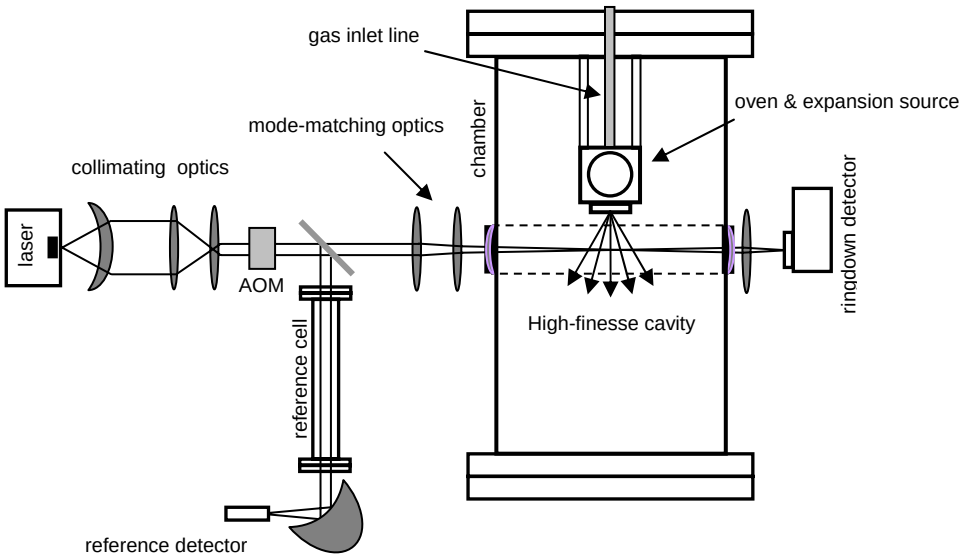

Figure 1: General experimental layout of the C_{60} experiment

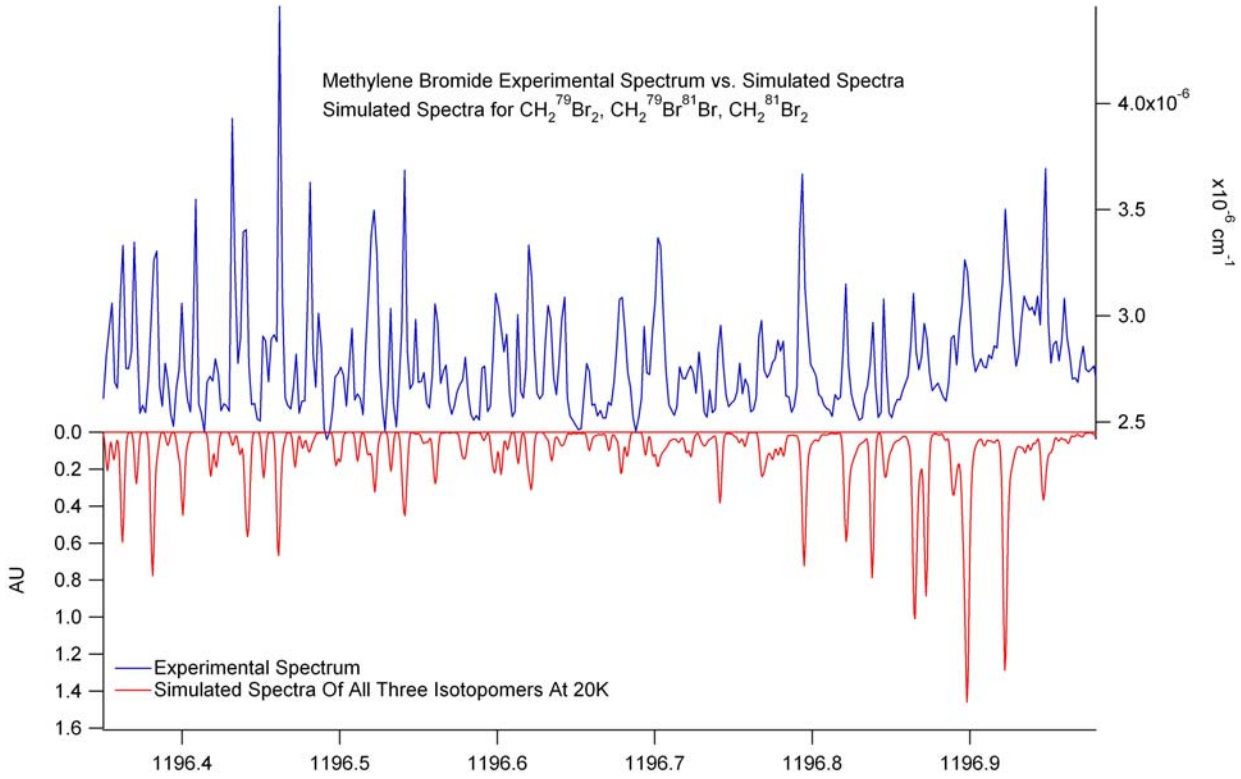

Figure 2: The top trace represents the experimental ringdown spectrum while the bottom trace represents a simulation of all three isotopomers run at a temperature of 20K.

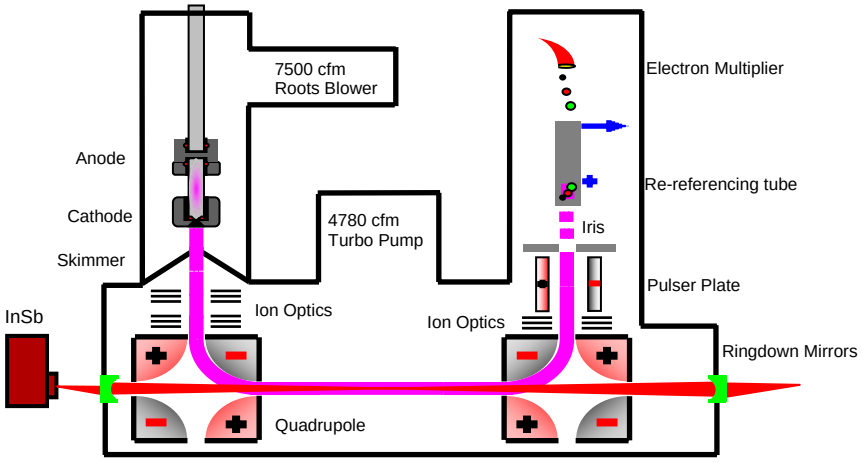

Figure 3: This figure provides the general layout of the SCRIBES instrument.

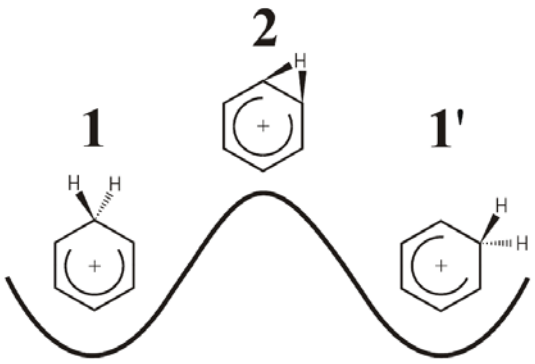

Figure 4: Diagram of benzenium ion equilbrium structure (1 and 1') and barrier crossing intermediate (2).

References

[1] Harter, W.G.; Reimer, T.C. *Chem. Phys. Lett.* **1992**, 194, 230.
[2] Sogoshi, N.; Kato, Y.; Wakabayashi, T.; Momose, T.; Tam, S.; DeRose, M.E.; Fajardo, M.E. *J. Chem. Phys. A.* **2000**, 104, 3733.
[3] Kroto, H.W.; Heath, J.R.; O'Brien, S.C.; Curl, R.F.; Smalley, R.E. *Nature*. **1985**, 318, 162.
[4] di Brozolo, F.R.; Bunch, T.E.; Fleming, R.H.; Macklin, J. *Nature*. **1994**, 369, 37.
[5] Becker, L.; Poreda, R.J.; Hunt, A.G.; Bunch, T.E.; Rampino, M. *Science*. **2001**, 291, 1530.
[6] Amirav, A.; Even, U.; Jortner, J. *Chem. Phys.* **1980**, 51, 31.
[7] Levy, D.; *Ann. Rev. Phys. Chem.* **1980**, 31, 197.
[8] Romanini, D.; Kachanov, A.A.; Sadeghi, N.; Stoeckel, F. *Chem. Phys. Lett.* **1997**, 264, 316.
[9] Romanini, D.; Kachanov, A.A.; Stoeckel, F. *Chem. Phys. Lett.* **1997**, 270, 538.
[10] Paldus, B.A.; Harb, C.C.; Spence T.G.; Zare, R.N.; Gmachl, G.; Capasso, F.; Sivco, D.L.; Baillargeon, J.N.; Hutchinson, A.L.; Cho, A.Y. *Opt. Lett.* **2000**, 25, 666.
[11] Kosterev, A.A.; Malinovsky, A.L.; Tittel, F.K.; Gmachl, C.; Capasso, F.; Sivco, D.L.; Baillargeon, J.N.; Hutchinson, A.L.; Cho, A.Y. *Appl. Opt.* **2001**, 40, 5522.
[12] Awtry, A.R.; Miller, J.H. *Appl. Phys. B.* **2002**, 75, 255.
[13] Sirtori, C.; Faist, J.; Capasso, F.; Cho, A.Y. *Pure Appl. Opt.* **1998**, 7, 373.
[14] Kosterev, A.A.; Tittel, F.K. *J. Quant. Electron.* **2002**, 38, 582.
[15] Barca-Galateanu, D. *Z. Phys.* **1941**, 117, 589.
[16] Craver, C.D., Ed. *Gases and Vapours*; The Coblentz Society: ,1980; p 32.
[17] Pgopher, A Program for Simulating Rotational Structure. C.M. Western, Univ. of Bristol. pgopher.chem.bris.ac.uk
[18] Davis, R.W.; Gerry, M.C.L.; *J. Mol. Spec.* **1985**, 109, 269.
[19] Niide, Y.; Tanaka, H.; Ohkoshi, I. *J. Mol. Spec.* **1990**, 139, 11.
[20] Smith, M.B.; March, J. *Advanced Organic Chemistry: Reactions, Mechanisms, and Structure, 5th Ed.*; Wiley: New York, 2001; pp 675-678.
[21] Olah, G.A.; Staral, J.S.; Asencio, G.; Liang, G.; Forsyth, G.D. *J. Am. Chem. Soc.* **1978**, 100, 6299.
[22] Olah, G.A.; Schlosberg, R.H.; Porter R.D.; Mo, Y.K.; Kelly, D.P.; Mateescu, G.D. *J. Am. Chem. Soc.* **1972**, 94, 2034.
[23] Solcá, N.; Dopfer, O. *Angew. Chem. Int. Ed.* **2002**, 41, 3628.
[24] Solcá, N.; Dopfer, O. *Chem. Eur. J.* **2003**, 9, 3154.
[25] Jones, W.; Boissel, P.; Chiavarino, B.; Cretoni, M.E.; Fornarini, S.; Lemaire, J.; Maitre, P. *Angew. Chem. Int. Ed.* **2003**, 42, 2057.
[26] Chiavarino, B.; Crestoni, M.E.; DePuy, C.H.; Fornarini, S.; Gareyev, R. *J. Phys. Chem.* **1996**, 100, 16201.
[27] Ascenzi, D.; Bassi, D.; Franceschi, P.; Tosi, P.; Di Stefano, M.; Rosi, M.; Sgamellotti, A. *J. Chem. Phys.* **2003**, 119, 8366.
[28] Schröder, D.; Loos, J.; Schwarz, H.; Thissen, R.; Dutuit, O. *J. Phys. Chem. A.* **2004**, 108, 9931.
[29] Maksić, Z.B.; Kovačević, B.; Lesar, A. *Chem. Phys.* **2000**, 253, 59.
[30] Sumathy, R.; Kryachko, E.S. *J. Phys. Chem. A.* **2002**, 106, 510.
[31] McEwan, M.J.; Scott, G.B.I.; Adams, N.G.; Babcock, L.M.; Terzieva, R.; Herbst, E. *Astrophys. J.* **1999**, 513, 287.
[32] Woods, P.; Millar, T.J.; Zulstra, A.A.; Herbst, E. *Astrophys. J.* **2002**, 574, L167.
[33] Cernicharo, J.; Heras, A.M.; Tielens, A.G.G.M; Pardo, J.R.; Herpin, F.; Guélin, M.; Waters, L.B.F.M. *Astrophys. J.* **2001**, 546, L123.
[34] Gudeman, C.S.; Begemann, M.H.; Pfaff, J.; Saykally, R.J. *Phys. Rev. Lett.* **1983**, 50, 727.
[35] Coe, J.V.; Owrutsky, J.C.; Keim, E.R.; Agman, N.V.; Hovde, D.C. *J. Chem. Phys.* **1989**, 90, 3893.
[36] Owrutsky, J.C.; Keim, E.R.; Coe, J.V.; Saykally, R.J. *J. Phys. Chem.* **1989**, 93, 5960.
[37] Keim, E.R.; Polak, M.L.; Owrutsky, J.C.; Coe, J.V.; Saykally, R.J. *J. Chem. Phys.* **1990**, 93, 3111.
[38] Kaufman, S.L. *Opt. Comm.* **1976**, 17, 309.
[39] Demtröder, W. *Laser Spectroscopy: Basic Concepts and Instrumentation*, 3rd ed.; Springer: Berlin, 2003; pp 553-555.
[40] Martínez, R.Z.; Metsälä, M.; Vaittinen, O.; Lantta, T.; Halonen, L. *J. Opt. Soc. Am. B.* **2006**, 23, 727.
[41] The GAP Group, GAP-Groups, Algorithms, and Programming, Version 4.4; 2007. www.gap-system.org.
[42] Bunker, P.R.; Jensen, P. *Molecular Symmetry and Spectroscopy, 2nd Ed.;* NRC Research Press: Ottawa,

Ontario, Canada, 1998; pp 82-89.

[43] Schmied, R.; Lehmann, K.K. *J. Mol. Spec*. **2004**, 226, 201.